

INORGANIC GEOCHEMICAL AND SEDIMENTOLOGICAL EVALUATION OF SOME SHALES IN THE CAMPANO-MAASTRICTIAN FORMATIONS OF ANAMBRA BASIN

¹M. E. Okiotor, ^{2*}O. I. Imasuen and ³D. E. Ogueh

¹Department of Geology & Petroleum Studies, Western Delta University, Oghara
¹michaelokiotor@gmail.com

²Department of Geology, University of Benin, Benin City

³Department of Geology & Petroleum Studies, Western Delta University, Oghara
 *Corresponding author: okpeseyi.imasuen@uniben.edu

Received: 18-05-17

Accepted: 25-07-17

ABSTRACT

This study presents an insight into the sediment provenance, paleoenvironment and conditions of deposition of Mamu Formation and Nkporo Group shales. To achieve this, sedimentologic and geochemical study of shale sequences from the Mamu and Nkporo group were carried out. Twenty five representative shale samples from these formations were subjected to sedimentologic, geochemical and mineralogical analyses using hydrometric method and Atomic Absorption Spectrophotometry (AAS). The results show that for the particles size analyses of sediments, the samples reveal medium grained with average sand, silt and clay values ranging from 33.1-54.7%, 29.08-52.1%, 8.0-16.48% respectively. The overall classification of the samples can be said to be poorly sorted sediments with low energy of deposition. The qualitative and quantitative analyses of the major elements namely SiO₂ (56.99% and 51.6%), Al₂O₃ (29.09% and 28.28%) and Fe₂O₃ (3.13% and 4.38%) for Mamu and Nkporo shales respectively indicate high detrital influx. While the positive correlation plots for SiO₂ against Al₂O₃, TiO₂ and K₂O are indicative of transported clay mineral units. The SiO₂/Al₂O₃ ratios observed for Nkporo shales can be said to be pure Kaolinite, while those for Mamu shales are both Kaolinite and Montmorrillonite.

Key words: sedimentologic, geochemical, shales, analyses, clay minerals.

INTRODUCTION

The Anambra Basin, is part of the Benue Trough, with a thick sequence of clastic sediments (approx. 6000m) ranging from bituminous shales, lignites through sandstones and marls and is stratigraphically positioned as the proto-Niger Delta (Nwajide and Reijers, 1997). It is one of the sedimentary basins in Nigeria with the potential to generate commercial accumulation of petroleum. As such it continues to generate and attract a lot of

research interests. Geochemical characterization has been a veritable tool in reconstruction of the paleoenvironment. The relationship between geochemical composition, sediment provenance and tectonic setting can be useful in extracting information from ancient rocks.

In order to further understand the sedimentologic, geochemical and mineralogical characters of the ancient sediments in this region there is the need to use a proven method of a geostatistical

approach used by Mostafa (2005) to analyse the geochemistry of the Cretaceous Abu Tartur Shales in Egypt thereby updating our knowledge of the Anambra basin sediments. Therefore this research focused on the sedimentological and geochemical characteristics, with intent to provide detailed information on the lithologies, textures, mineralogical compositions and the geostatistical signatures of the major oxides in order to establish the paleo-depositional environment and conditions of these organic rich sediments.

Geological Setting

The origin of many sedimentary basins in West Africa, including that of the Anambra Basin, is associated with the splitting-up of the Gondwana supercontinent (Nwajide and Reijers, 1996). The Anambra Basin, which constitutes the southern portion of the Benue Trough is one of the intercratonic Cretaceous Basins linked to the Benue Trough in Central and West Africa and whose origin is related to the separation of Africa from South America and the opening

of the South Atlantic Ocean (Ofoegbu et al, 1990; Obaje et al, 2004.). It contains sediments of over 9km in thickness and 402.34Km long extending in a NE-SW direction between Onitsha on the Niger River and Kwande on the Benue River (Whiteman, 1982).

The Anambra Basin proper formed after the Santonian tectonic pulse, dating back to 84my. During the Albian-Santonian, the Benue Trough, with the Abakaliki and Benue basins, was essentially an intracratonic mobile sedimentary basin, whereas the proto-Anambra basin was a platform only thinly draped by older sediments. During the Santonian compressional event the Abakaliki basin folded and was uplifted and a westward translation of the depocentre took place towards the Anambra basin (Nwajide and Reijers, 1996). Sediments were derived from the uplands beyond the Benue hinge line, the Abakaliki uplands and Benue fold belt.

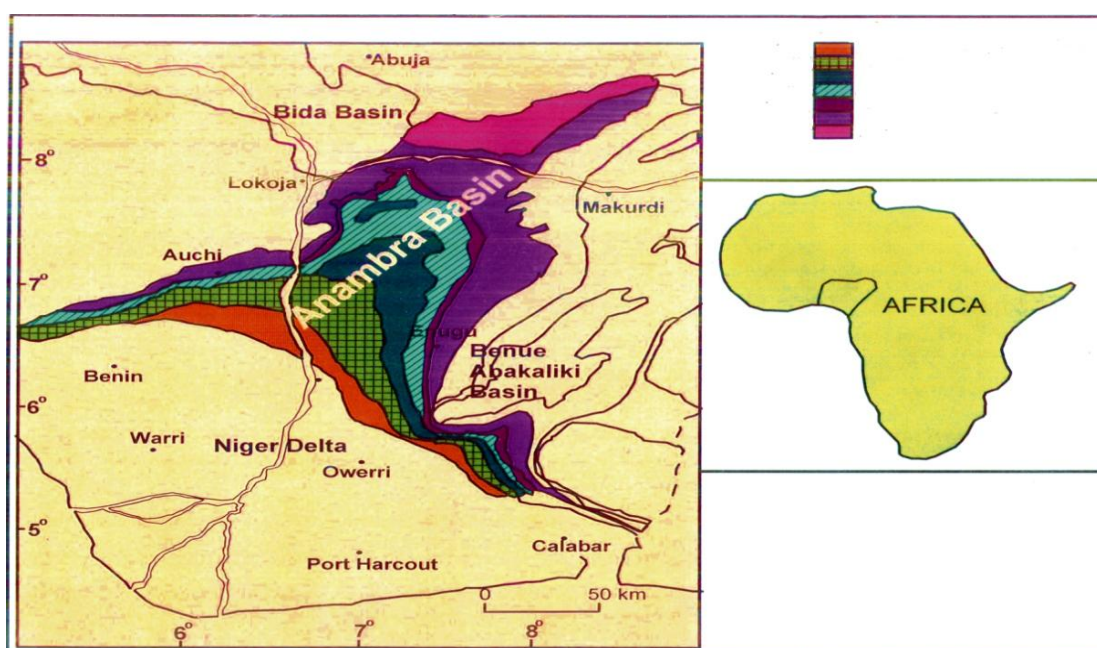


Figure 1. Anambra Basin showing the extent of the Nkporo group and the Mamu Formation (After Adekoya, 2011)

MATERIALS AND METHODS

Methods of investigation involved both field study and laboratory analyses. Intensive field study covered a total of 6 localities from where 25 samples were taken (Fig. 2). The exposure were at Onyeama Mine Road (Proda), Onyeama Mine, Trans – Ekulu (Agu-Abor on Enugu-Onitsha Express

way), Umonaw, Four – Corner Junction (Ozalla) and Agbogugu. The samples collected at these exposures were analyzed for their sedimentologic and geochemical characteristics. Also bedding characteristics in terms of structure, texture, attitude and lithology were studied and described.

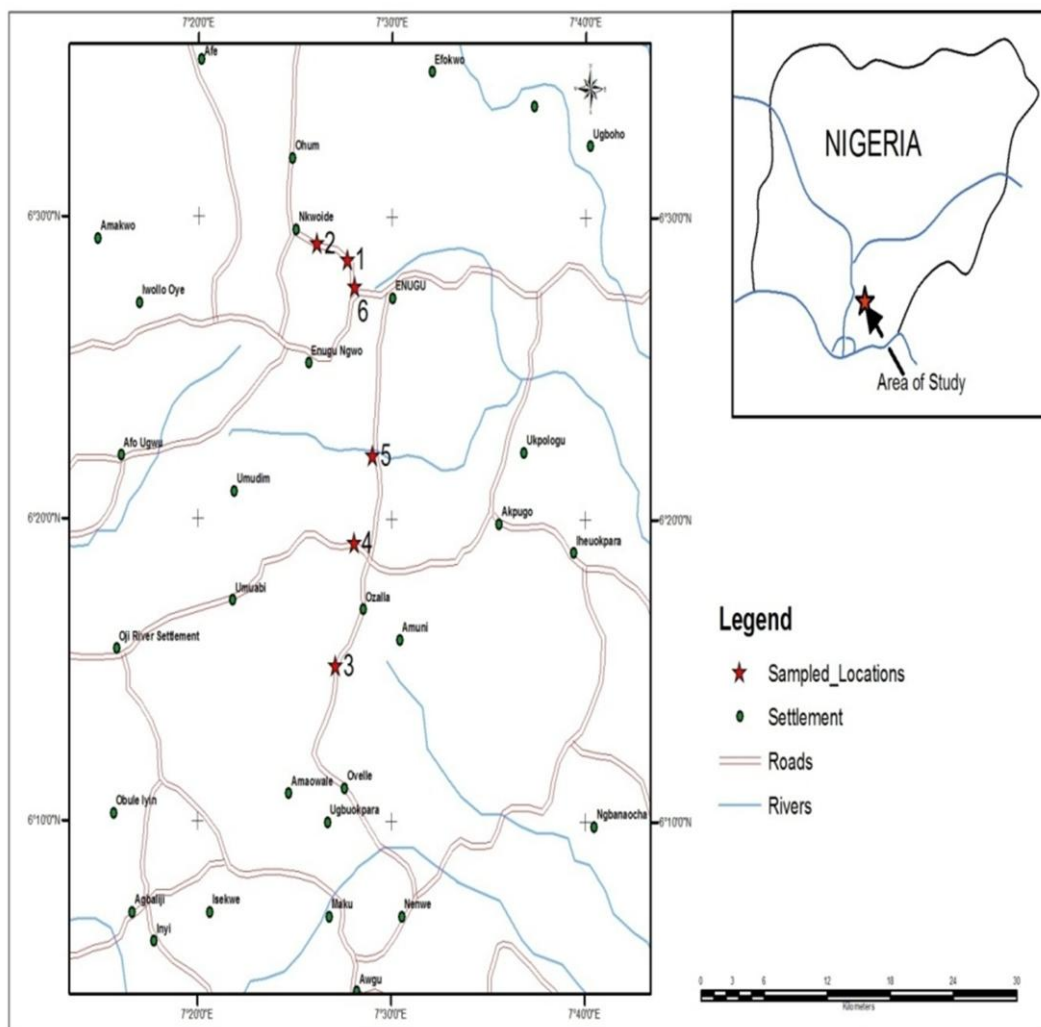


Figure 2. Map of Enugu and Environs showing the sampled locations



Plate 1. Shale exposure at Umonaw on Enugu Port-Harcourt Expressway

Laboratory studies of the samples were based on grain size analysis using Hydrometric Method. This is particle size (mechanical) analysis using Bouyoucos and hydrometer method

5gm of fine texture soil was weighed and placed in the baffled cup. The cup was filled to half full with distilled water and 10ml of calgon (sodium hexametaphosphate) was added. The cup was placed on stirrer and stirred until soil aggregates were broken down (15 mins). The suspension was transferred to a bouyoucos cylinder and was filled to the lower mark with distilled water while the hydrometer was in suspension. The first reading on the hydrometer was taken at 40 seconds after the cylinder was set down, the hydrometer removed and

temperature of suspension recorded with a thermometer. After the first hydrometer reading, the suspension was allowed to stand for 3 hours and a second reading taken as well as the temperature of the suspension. The first reading measured the temperature of sand and clay in suspension, the second reading indicated the percentages of 2 micron (total clay in suspension). The results were corrected to a temperature of 68°F. For every degree over 68°F, 0.2 was added to hydrometer reading before computation. And for under 68°F 0.2 was subtracted from hydrometer reading. Extremes such as 50°F or 100°F were avoided. Also 2.0 was subtracted from every hydrometer reading to compensate for the added dispersing agent.

Sample Calculations:

Given: (1a) Hydrometer reading at 40seconds, $H_1 = 18$

(1b) Temperature at 40 seconds $T_1 = 750^\circ\text{F}$

(2a) Hydrometer reading at 3 hours, $H_2 = 8$

(3) Temperature correction to be added to hydrometer reading $= 0.2 (T-68)$

Where $T =$ degrees Fahrenheit.

(4) Salt correction to be added to hydrometer reading $= 2.0$.

Calculations:

$$A \text{ SAND} = 100.0 - (H_1 + 0.2(T_1 - 68 - 2.0) / 2) = 65.2\%$$

$$B \text{ CLAY} = (H_2 + 0.2(T_2 - 68) / 2) = 10.0\%$$

$$C \text{ SILT} = 100.0 - (\% \text{ sand} + \% \text{ clay}) = 24.8\%$$

The class name or texture of the soil was determined from the textural triangle (Fig. 3).

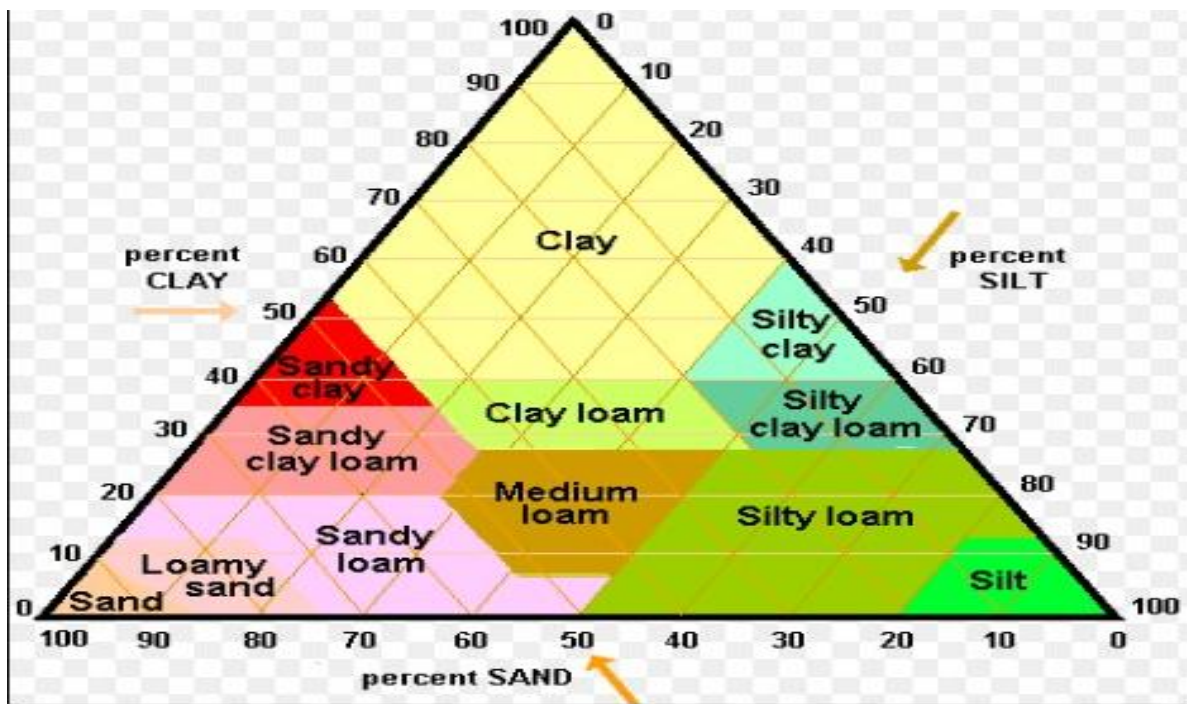


Figure 3. USDA (The United States Department of Agriculture) Textural Triangle

The geochemical analyses to determine the major oxides were done using the Atomic Absorption Spectrophotometer (AAS) Method. Atomic absorption spectrophotometer is the instrument used for Atomic Absorption Spectrometry, hence the name, varieties of which are available in our modern markets. The AAS operates on the basis of the fact that atoms of an element

can absorb electromagnetic radiation. This occurs when the element is atomized and the wavelength absorbed is specific to each element.

The Unicam 929aa spectrometer was used in this research. The machine comprises a source of radiation which is a hollow cathode ray lamp, an atomizing device i.e.

the burner sample compartment, a monochromator, a detector and a measuring system or meter. The radiation produced by the hollow cathode ray lamp corresponds to the emission spectrum of that element hence the required line may be isolated by the monochromator. The advantages of the AAS are accounted for by its high sensitivity, practical absence of spectral interference, operation simplicity and reasonable cost o equipment.

The results emanating from these were then subjected to geostatistical analysis such as pearson correlation to reveal the hidden similarities and dissimilarities between the

sediments. Elemental ratio analyses was also done to determine the clay content of the sediments.

RESULTS AND DISCUSSION

The hydrometric analysis shows that the sediments are medium grained with average sand, silt, and clay values ranging from 33.1-54.7%, 29.08-52.1%, 8-43.8 (Table 1). These shows poorly sorted sediments with low energy of deposition. The high percentage of sand with silts indicates a swampy environment with moderately low energy, indicating that these sediments might have been deposited under marginal marine environment.

Table 1: Results of particle size analysis

S/N	Sample Code	% Clay	% Silt	% Sand
1	AGG 3	43.8	18.7	37.5
2	AGG 1	39.4	20.4	40.2
3	UM 1.5	2.5	52	45.5
4	UM 1.8	3.9	42.9	53.2
5	UM 2.5	5.7	46.8	47.5
6	UM 1.2	11.3	40.9	47.8
7	UM 2.2	8.8	46.7	44.5
8	FCJ 1.5	6.5	37.8	55.7
9	FCJ 2.3	4.9	51.6	43.5
10	FCJ 1.2	7.1	42	50.9
11	FCJ 2.1	3.8	43.8	52.4
12	TE 2	12.7	55.4	31.9
13	TE 4	27.6	42.7	29.7
14	T E 8	9.8	61.6	28.6
15	T E 7	11.4	46.1	42.5
16	T E 11	10.7	49.6	39.7
17	T E 15	16.4	57.3	26.3
18	OM 1	6.5	51.7	41.8
19	OM 2	9.8	45.6	44.6
20	OM 4	7.7	52.6	39.7
21	OMR 2	14.5	28.4	57.1
22	OMR 4	18.3	25.9	55.8
23	OMR 7	15.5	34.7	49.8
24	OMR 9	17.9	30.4	51.7
25	OMR 11	14.8	26	59.2

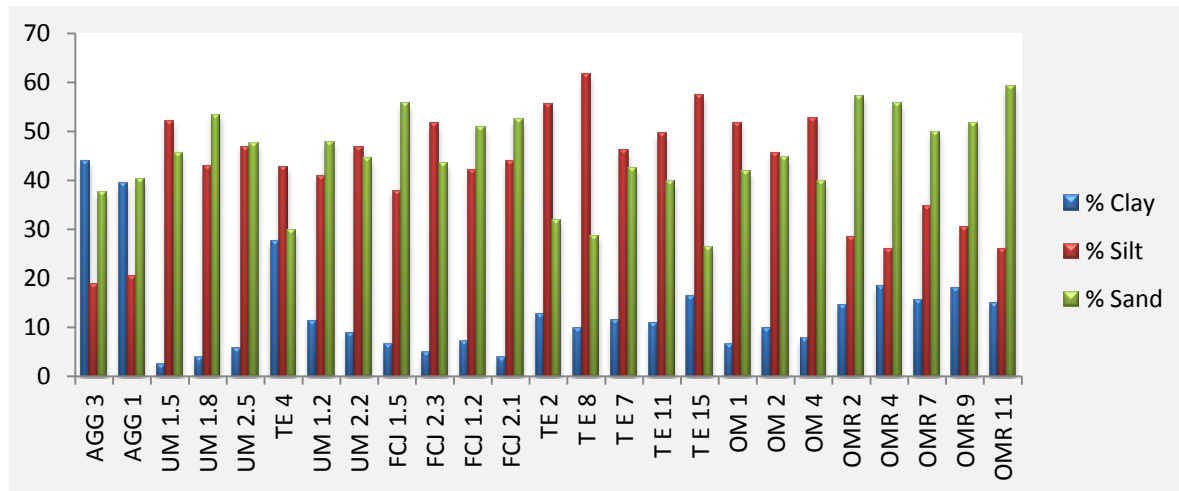


Figure 4 Histogram plot of the particle size analyses

The averages of major and trace element for the studied formations are shown in Tables 2 and 3. The major elements determined are SiO_2 , Al_2O_3 , Fe_2O_3 , CaO , MgO , Na_2O , MnO , NiO_2 and TiO_2 . The trace elements are Pb, Zn, Cu, Ba, Cr, Ni, Cd, As, Se and V.

Table 2: The Major and Trace element averages for the studied locations of Mamu shales

	OMR 2	OMR 4	OMR 7	OMR 9	OMR 11	OM 1	OM 2	OM 4	Averages
SiO₂	65.12	68.02	55	66.21	65.4	48.2	42.3	45.6	56.99
Al₂O₃	32.33	33.12	30.1	28.58	29.3	26.3	24.7	28.3	29.09
Fe₂O₃	3.74	5.68	4.58	2.05	2.96	2.85	1.69	1.52	3.13
MgO	0.05	0.07	0.04	0.25	0.06	0.06	0.08	0.06	0.08
CaO	1.09	0.05	3.51	1.72	1.07	0.39	0.44	0.44	1.09
Na₂O	2.84	2.62	3.59	2.91	2.1	2.24	2.09	2.16	2.57
K₂O	2.27	2.33	2.47	2.03	1.71	2.22	1.65	1.42	2.01
MnO	0.34	0.45	0.52	0.86	0.20	0.65	0.35	0.32	0.46
NiO₂	0.40	0.69	0.38	0.40	0.17	0.2	0.39	0.2	0.35
TiO₂	2.75	2.21	2.05	2.45	2.11	3.22	3.21	3.15	2.64
Pb	25	37	47.5	39	25	ND	35	20.5	28.63
Zn	1.3	1.26	0.18	1.33	1.26	1.1	1.14	1.06	1.08
Cu	9	16	41.5	16.5	24.5	9.5	11.5	18.5	18.38
Ba	ND	ND	ND	ND	ND	ND	ND	ND	0.00
Cr	0.053	0.052	0.056	0.093	0.04	0.03	0.06	0.06	0.06
Ni	13	44.5	24.5	26	11.5	13	25.5	30.5	23.56
Cd	ND	ND	ND	ND	ND	ND	ND	ND	0.00
As	5.22	4.26	5.81	3.88	2.71	20.4	8.14	15.9	8.29
Se	25.02	30.3	26.15	3.32	11.6	4.57	2.08	9.3	14.05

Silica (SiO₂)

Silica is the dominant constituent of all the shale samples, this because silica form the framework for the constituent silicate minerals in these shales. The average content of silica in the samples from Mamu Formation and Nkporo Group are 56.99% and 51.67% respectively. This range is in conformity with the average shales of Pettijohn (1975) of 58.50%. The only exception is in the Umonaw shales where the average silica content is 76.25%.

Silica has a weak positive correlation with Al₂O₃, TiO₂ and K₂O, therefore SiO₂ is considered to be dominantly terrigenous in origin which is shown in the scatter plots of SiO₂ with Al₂O₃, TiO₂ and K₂O (Fig 3 & 4). This is also reflected in the weak positive correlation matrix in the majority of the samples studied in that $0.074 \leq r \leq 0.65$, with the exception of $r = 0.74$ & 0.75 ($r^2 = 56\%$) at Trans Ekulu (Table 5). This indicates that the SiO₂ were terrigenous and there was some association with the Al₂O₃, TiO₂ & K₂O in their depositional process. This tends to agree with Agumanu (1993), who stated that sediments within the Anambra basin show remarkable textural and mineralogical maturity indicating that their sources were both from previously deposited sediment and possibly intensely in-situ chemically weathered crystalline basement rock. Perhaps part of the silica may also have been contributed due to a

biogenic origin by silica secreting organisms. Silica may also be precipitated as cement filling cavities. The silica may occur as quartz disseminated with kaolinite, or deposited with the tiny flakes of the clay minerals (Bain and Smith, 1987; Moore and Reynolds, 1997). On the average, the silica content in the studied shales correlated essentially positively with Al₂O₃ for both formations (Table 8). This indicates that SiO₂ is mainly present in the studied shales as part of the clay minerals and detrital silicate.

Felix (1977) reported that the SiO₂/Al₂O₃ ratio for pure montmorillonite ranges from 2.80 to 3.31 while for pure kaolinite it is about 1.18. In the studied samples, the Mamu shales in the Onyeama mine area (OM) are kaolinite with SiO₂/Al₂O₃ ratio ranging from 1.61 to 1.83 with an average of 1.72, while those in the Onyeama Mine road, OMR (Proda: Under the bridge) are mixed montmorillonite and kaolinite clays with SiO₂/Al₂O₃ ratios between 1.83 and 2.32. For the Nkporo Group, the SiO₂/Al₂O₃ ratio reveal that the shales from Trans Ekulu (TE), Four Corner junction (FCJ) or Ozalla junction and Agbogugu are all made up of Kaolinite clays with SiO₂/Al₂O₃ ratios ranging from 0.82 – 1.71 (Table 10). While the shales from Umonaw can be said to be pure montmorillonite clays with SiO₂/Al₂O₃ ratio between 2.75 and 3.37, in accordance with Felix (1977).

Table 4: Correlation matrix of major Oxides from Onyema mine road (OMR)

	% SiO ₂	% Al ₂ O ₃	% Fe ₂ O ₃	% MgO	% CaO	% K ₂ O	% Na ₂ O	% MnO	% NiO ₂	% TiO ₂
OMR 2	65.12	32.33	3.74	0.05	1.09	2.27	2.84	0.34	0.40	2.75
OMR 4	68.02	33.12	5.68	0.07	0.05	2.33	2.62	0.45	0.69	2.21
OMR 7	55	30.1	4.58	0.04	3.51	2.47	3.59	0.52	0.38	2.05
OMR 9	66.21	28.58	2.05	0.25	1.72	2.03	2.91	0.86	0.40	2.45
OMR 11	65.41	29.32	2.96	0.06	1.07	1.71	2.1	0.20	0.17	2.11

	% SiO ₂	% Al ₂ O ₃	% Fe ₂ O ₃	% MgO	% CaO	% K ₂ O	% Na ₂ O	% MnO	% NiO ₂	% TiO ₂
% SiO ₂	1	0.26	-0.16	0.35	-0.93	-0.47	-0.77	-0.04	0.27	0.42
% Al ₂ O ₃	0.26	1	0.81	-0.55	-0.53	0.56	-0.03	-0.39	0.71	0.27
% Fe ₂ O ₃	-0.16	0.81	1	-0.67	-0.16	0.69	0.22	-0.32	0.69	-0.31
% MgO	0.35	-0.55	-0.67	1	-0.02	-0.29	0.00	0.85	0.03	0.25
% CaO	-0.93	-0.53	-0.16	-0.02	1	0.33	0.78	0.30	-0.38	-0.30
% K ₂ O	-0.47	0.56	0.69	-0.29	0.33	1	0.81	0.23	0.66	0.07
% Na ₂ O	-0.77	-0.03	0.22	0.00	0.78	0.81	1	0.51	0.23	-0.02
% MnO	-0.04	-0.39	-0.32	0.85	0.30	0.23	0.51	1	0.30	0.14
% NiO ₂	0.27	0.71	0.69	0.03	-0.38	0.66	0.23	0.30	1	0.10
% TiO ₂	0.42	0.27	-0.31	0.25	-0.30	0.07	-0.02	0.14	0.10	1
Pb	-0.61	-0.18	0.28	0.20	0.64	0.61	0.79	0.64	0.37	-0.47
Zn	0.97	0.14	-0.35	0.39	-0.86	-0.57	-0.78	-0.06	0.08	0.55
Cu	-0.87	-0.40	0.17	-0.29	0.80	0.21	0.51	0.00	-0.29	-0.80
Cr	0.09	-0.42	-0.49	0.91	0.22	0.09	0.39	0.97	0.19	0.33
Ni	0.19	0.43	0.63	0.15	-0.27	0.49	0.18	0.40	0.90	-0.28
As	-0.64	0.38	0.46	-0.31	0.54	0.93	0.89	0.19	0.36	0.20
Se	-0.25	0.86	0.94	-0.78	-0.08	0.75	0.30	-0.43	0.57	-0.08

Table 5: Correlation matrix of major oxides from Trans Ekulu (TE)

	Distance	% SiO ₂	% Al ₂ O ₃	% Fe ₂ O ₃	% MgO	% CaO	% K ₂ O	% Na ₂ O	% MnO	% NiO ₂	% TiO ₂
TE 2	45.7	44	32.12	2.69	0.15	1.01	2.79	2.49	0.46	0.28	4.25
TE 4	45.71	48	31.25	6.11	0.14	2.89	3.21	4.64	0.37	0.18	4.56
TE 7	45.72	38.25	30.12	3.58	0.09	1.42	2.1	2.77	0.52	0.25	4.68
TE 8	45.73	38.12	28.48	9.06	0.06	4.91	2.25	3.04	0.61	0.51	4.01
TE 11	45.74	41.58	29.74	5.56	0.05	3.51	1.66	2.04	0.47	0.38	4.32
TE 15	45.75	42.44	30.12	3.30	0.1	4.21	2.28	3.17	0.27	0.32	4.08

	% SiO ₂	% Al ₂ O ₃	% Fe ₂ O ₃	% MgO	% CaO	% K ₂ O	% Na ₂ O	% MnO	% NiO ₂	% TiO ₂
% SiO ₂	1	0.74	-0.21	0.73	-0.20	0.75	0.60	-0.65	-0.66	0.21
% Al ₂ O ₃	0.74	1	-0.69	0.91	-0.77	0.66	0.20	-0.46	-0.79	0.39
% Fe ₂ O ₃	-0.21	-0.69	1	-0.51	0.69	-0.06	0.25	0.54	0.62	-0.30
% MgO	0.73	0.91	-0.51	1	-0.61	0.88	0.49	-0.45	-0.75	0.28
% CaO	-0.20	-0.77	0.69	-0.61	1	-0.29	0.14	-0.03	0.68	-0.66
% K ₂ O	0.75	0.66	-0.06	0.88	-0.29	1	0.78	-0.31	-0.58	0.19
% Na ₂ O	0.60	0.20	0.25	0.49	0.14	0.78	1	-0.37	-0.48	0.25
% MnO	-0.65	-0.46	0.54	-0.45	-0.03	-0.31	-0.37	1	0.55	-0.01
% NiO ₂	-0.66	-0.79	0.62	-0.75	0.68	-0.58	-0.48	0.55	1	-0.76
% TiO ₂	0.21	0.39	-0.30	0.28	-0.66	0.19	0.25	-0.01	-0.76	1
Pb	-0.10	0.02	-0.01	0.40	0.02	0.50	0.46	-0.03	-0.05	-0.18
Zn	0.69	0.13	0.17	0.03	0.29	0.18	0.45	-0.53	-0.32	0.19
Cu	-0.43	-0.54	0.77	-0.40	0.45	-0.12	-0.18	0.76	0.82	-0.58
Cr	-0.25	0.12	-0.22	-0.03	-0.15	-0.25	-0.75	0.27	0.47	-0.58
Ni	-0.66	-0.79	0.61	-0.75	0.69	-0.58	-0.47	0.54	1.00	-0.77
As	-0.28	-0.57	0.81	-0.20	0.57	0.21	0.43	0.46	0.50	-0.36
Se	0.17	-0.07	-0.27	0.05	0.29	0.03	0.43	-0.76	-0.35	0.08

Table 6: Correlation matrix of major oxides from Umonaw (UM)

	Distance	% SiO ₂	% Al ₂ O ₃	% Fe ₂ O ₃	% MgO	% CaO	% K ₂ O	% Na ₂ O	% MnO	% NiO ₂	% TiO ₂
UM 1.2	42.8	75.58	22.45	3.14	0.13	1.49	2.55	3.38	0.34	0.34	4.15
UM 1.5	42.81	77.25	25.12	4.66	0.55	0.36	3.21	4.79	0.41	0.31	3.25
UM 1.8	42.82	72	26.22	3.80	0.05	6.18	2.09	2.9	0.45	0.32	3.12
UM 2.2	42.83	76.4	23.45	3.66	0.08	0.3	1.66	2.3	0.34	0.34	3.05
UM 2.5	42.84	80	24.12	4.60	0.13	0.43	2.66	3.71	0.39	0.22	3.58

	% SiO ₂	% Al ₂ O ₃	% Fe ₂ O ₃	% MgO	% CaO	% K ₂ O	% Na ₂ O	% MnO	% NiO ₂	% TiO ₂
% SiO ₂	1	-0.41	0.57	0.32	-0.86	0.42	0.42	-0.38	-0.69	0.22
% Al ₂ O ₃	-0.41	1	0.51	0.20	0.63	0.11	0.20	0.96	-0.16	-0.68
% Fe ₂ O ₃	0.57	0.51	1	0.60	-0.29	0.58	0.66	0.49	-0.72	-0.39
% MgO	0.32	0.20	0.60	1	-0.42	0.81	0.88	0.19	-0.03	-0.09
% CaO	-0.86	0.63	-0.29	-0.42	1	0.30	-0.31	0.68	0.22	-0.21
% K ₂ O	0.42	0.11	0.58	0.81	-0.30	1	0.99	0.25	-0.37	0.36
% Na ₂ O	0.42	0.20	0.66	0.88	-0.31	0.99	1	0.31	-0.36	0.21
% MnO	-0.38	0.96	0.49	0.19	0.68	0.25	0.31	1	-0.26	-0.46
% NiO ₂	-0.69	-0.16	-0.72	-0.03	0.22	0.37	-0.36	-0.26	1	-0.07
% TiO ₂	0.22	-0.68	-0.39	-0.09	-0.21	0.36	0.21	-0.46	-0.07	1
Pb	0.00	-0.26	-0.12	0.56	-0.47	0.07	0.14	-0.42	0.66	-0.19
Zn	-0.50	0.11	-0.37	-0.13	0.61	0.28	0.18	0.32	0.11	0.59
Cu	-0.52	-0.48	-0.92	-0.53	0.14	0.73	-0.77	-0.57	0.81	0.08
Cr	-0.06	-0.19	-0.26	-0.36	-0.20	0.80	-0.72	-0.43	0.37	-0.56
Ni	-0.66	-0.19	-0.73	-0.03	0.19	0.38	-0.36	-0.30	1.00	-0.05
As	0.26	-0.07	0.25	0.50	-0.58	0.05	0.07	-0.30	0.30	-0.55

Table 7: Correlation matrix quick view of the major elements

OMR	r	100r ²	OM	r	100r ²	FCJ	r	100r ²	UM	r	100r ²	TE	R	100r ²
SiO ₂ vs. Al ₂ O ₃	0.26	6.62	SiO ₂ vs. Al ₂ O ₃	0.51	25.92	SiO ₂ vs. Al ₂ O ₃	0.45	19.9	SiO ₂ vs. Al ₂ O ₃	-0.41	16.63	SiO ₂ vs. Al ₂ O ₃	0.74	54.07
SiO ₂ vs. TiO ₂	0.42	17.37	SiO ₂ vs. TiO ₂	0.07	0.54	SiO ₂ vs. TiO ₂	-0.57	32.97	SiO ₂ vs. TiO ₂	0.22	4.93	SiO ₂ vs. TiO ₂	0.21	4.58
SiO ₂ vs. K ₂ O	-0.47	22.48	SiO ₂ vs. K ₂ O	0.65	42.05	SiO ₂ vs. K ₂ O	0.54	28.67	SiO ₂ vs. K ₂ O	0.42	17.98	SiO ₂ vs. K ₂ O	0.75	56.34
Al ₂ O ₃ vs. TiO ₂	0.27	7.38	Al ₂ O ₃ vs. TiO ₂	-0.82	67.37	Al ₂ O ₃ vs. TiO ₂	-0.98	96.23	Al ₂ O ₃ vs. TiO ₂	-0.68	45.57	Al ₂ O ₃ vs. TiO ₂	0.39	15.14
CaO vs. K ₂ O	0.33	10.59	CaO vs. K ₂ O	-0.96	92.2	CaO vs. K ₂ O	-0.43	18.52	CaO vs. K ₂ O	-0.30	9.28	CaO vs. K ₂ O	-0.29	8.23
Ni vs. Al ₂ O ₃	0.43	18.38	Ni vs. Al ₂ O ₃	0.32	10.45	Ni vs. Al ₂ O ₃	0.27	7.46	Ni vs. Al ₂ O ₃	-0.19	3.7	Ni vs. Al ₂ O ₃	-0.79	63.14
Al ₂ O ₃ vs. K ₂ O	0.56	31.11	Al ₂ O ₃ vs. K ₂ O	-0.33	10.56	Al ₂ O ₃ vs. K ₂ O	0.81	65.53	Al ₂ O ₃ vs. K ₂ O	0.11	1.21	Al ₂ O ₃ vs. K ₂ O	0.66	42.97
CaO vs. Na ₂ O	0.78	61.44	CaO vs. Na ₂ O	-0.88	78.25	CaO vs. Na ₂ O	-0.49	23.63	CaO vs. Na ₂ O	-0.31	9.84	CaO vs. Na ₂ O	0.14	2.1
Cr vs. Al ₂ O ₃	-0.42	17.95	Cr vs. Al ₂ O ₃	-0.01	0.01	Cr vs. Al ₂ O ₃	-0.09	0.83	Cr vs. Al ₂ O ₃	-0.19	3.78	Cr vs. Al ₂ O ₃	0.12	1.36
Na ₂ O vs. K ₂ O	0.81	65.24	Na ₂ O vs. K ₂ O	0.72	51.73	Na ₂ O vs. K ₂ O	0.99	97.37	Na ₂ O vs. K ₂ O	0.99	97.54	Na ₂ O vs. K ₂ O	0.78	60.75
Ni vs. NiO ₂	0.90	80.76	Ni vs. NiO ₂	0.24	5.77	Ni vs. NiO ₂	1.00	99.31	Ni vs. NiO ₂	1.00	99.87	Ni vs. NiO ₂	1.00	99.95

Table 8: Summary of Coefficient of determination of the oxides

	OMR	OM	FCJ	UM	TE
SiO ₂ vs. Al ₂ O ₃	6.62	25.92	19.9	16.63	54.07
SiO ₂ vs. TiO ₂	17.37	0.54	32.97	4.93	4.58
SiO ₂ vs. K ₂ O	22.48	42.05	28.67	17.98	56.34
Al ₂ O ₃ vs. TiO ₂	7.38	67.37	96.23	45.57	15.14
CaO vs. K ₂ O	10.59	92.2	18.52	9.28	8.23
Ni vs. Al ₂ O ₃	18.38	10.45	7.46	3.7	63.14
Al ₂ O ₃ vs. K ₂ O	31.11	10.56	65.53	1.21	42.97
CaO vs. Na ₂ O	61.44	78.25	23.63	9.84	2.1
Cr vs. Al ₂ O ₃	17.95	0.01	0.83	3.78	1.36
Na ₂ O vs. K ₂ O	65.24	51.73	97.37	97.54	60.75
Ni vs. NiO ₂	80.76	5.77	99.31	99.87	99.95

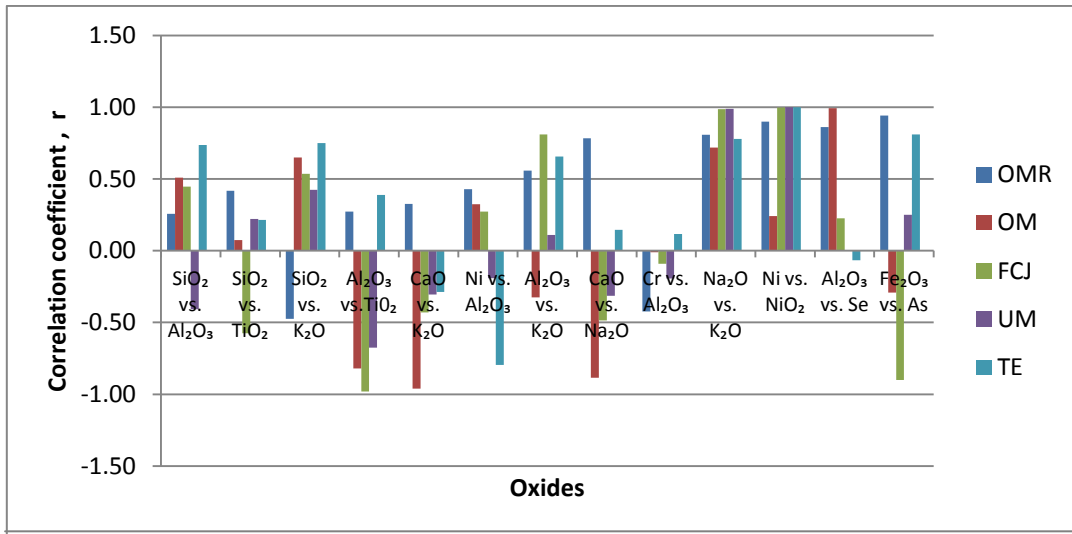


Figure 5. Histogram of correlation of the major elements

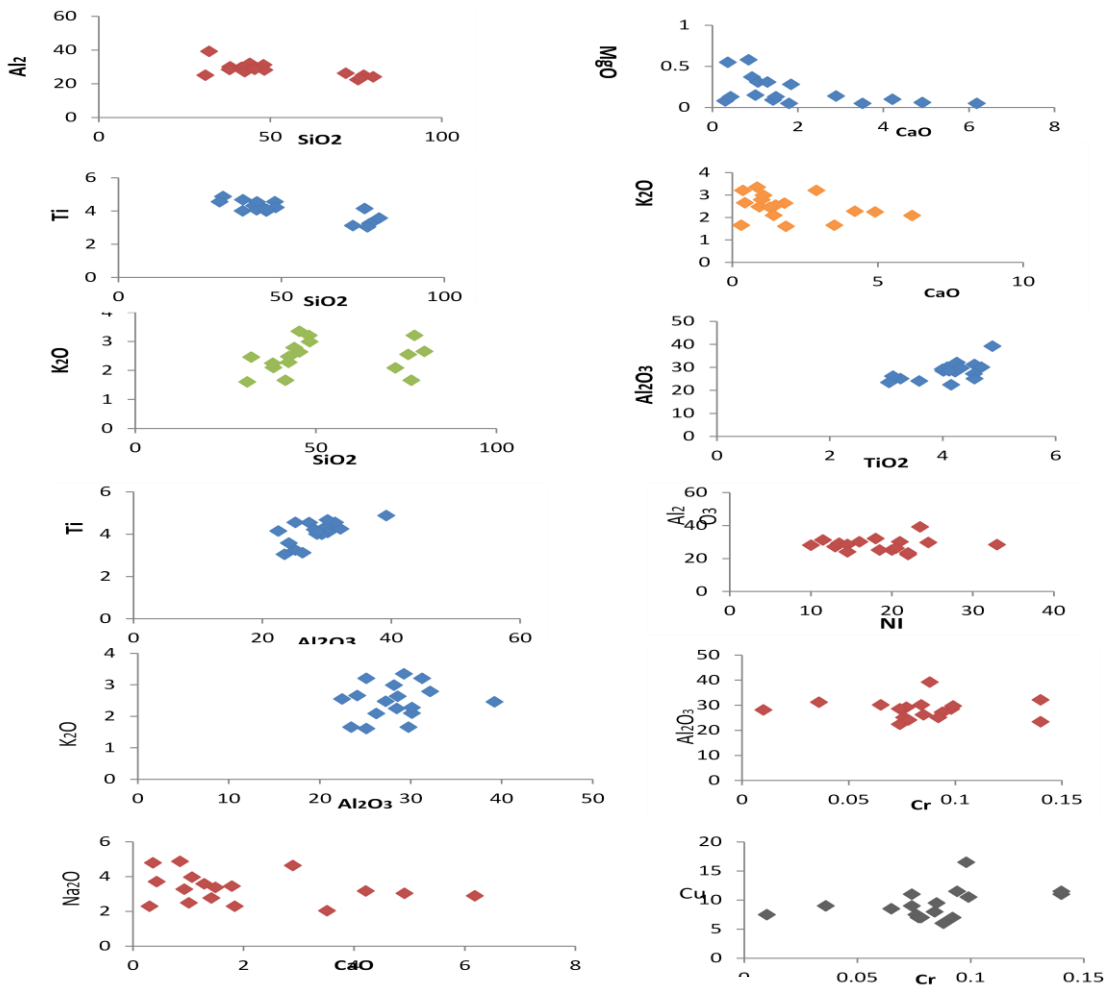


Figure 6: Scatter plots of major elements of Nkporo

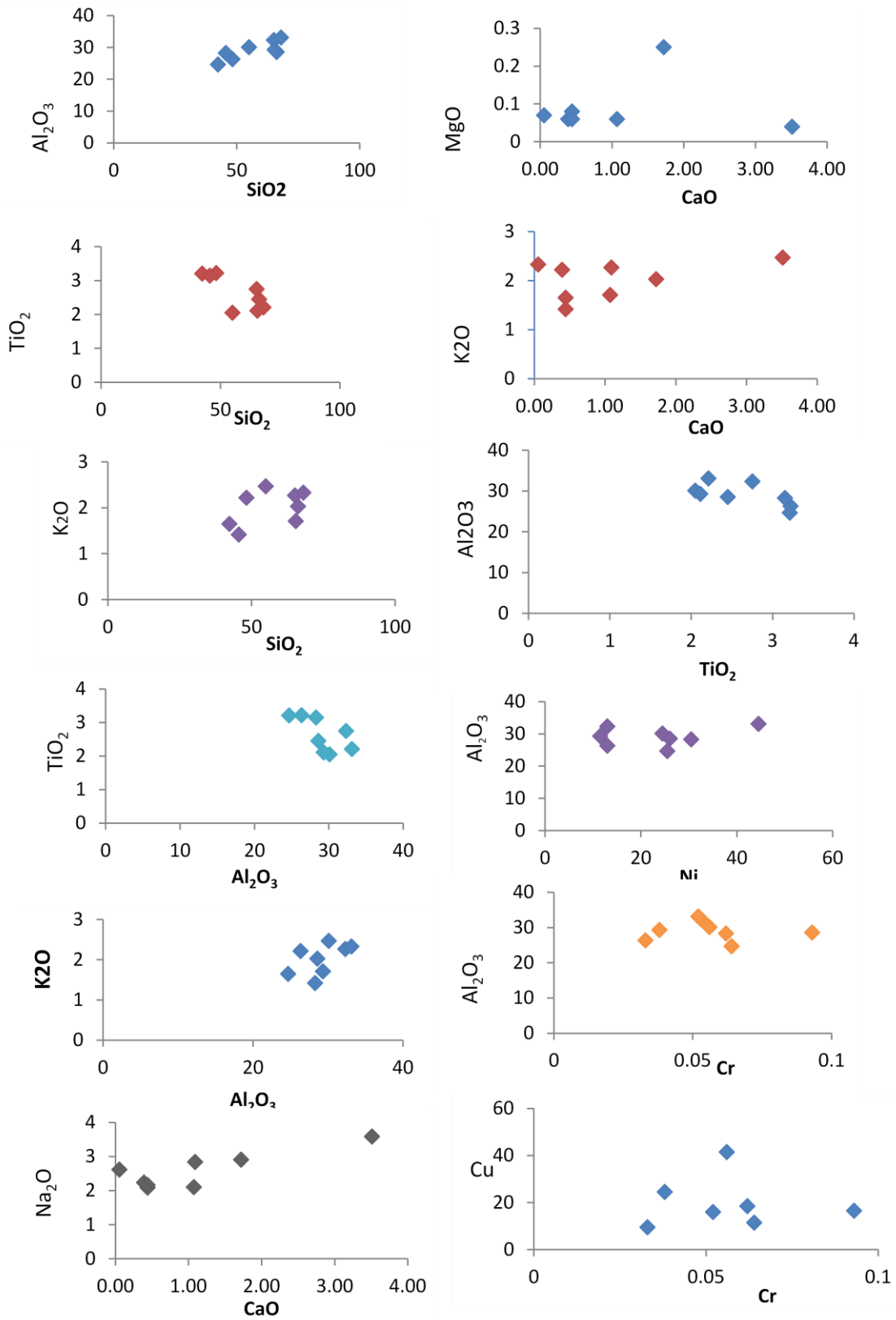


Figure 7: Scatter Plots of Major oxides of Nkporo Group

Table 9: SiO₂/Al₂O₃ ratio for Mamu & Nkporo shale

	SiO₂/Al₂O₃ ratio	Inference
Mamu shales	1.61-2.32	Kaolinite and montmorillonite
Nkporo group shales	0.82 – 1.71	Kaolinite
Umonaw	2.75 - 3.37	Pure montmorillonite

Iron Oxide (Fe₂O₃)

The average content of Fe₂O₃ in the shale samples is 3.13% and 4.38% for Mamu and Nkporo Group respectively. They are close to the averages of 4.72% and 4.80% for Pettijohn (1975) and Mostafa (2005) respectively. Iron is present in the structure of clay minerals and/or as an independent Fe-Mineral such as goethite. According to Sharma (1979), in the marine environment, the hydroxides of iron are carried as particles and colloids in suspension and therefore, tends to aggregate in the fine fraction of sediments.

The enrichment of iron in the studied shales may be attributed to their formation under more reducing conditions with a high input of non-reactive iron to the basin (Ahmed, 1997).

There is generally, a positive moderate correlation between Fe₂O₃ and the SiO₂ (r=0.57), Al₂O₃ (r=0.51), MgO (r=0.60), Na₂O (r=0.66) (Table 6). This may be due to the association of Fe³⁺ with clay minerals (Mostafa, 2005).

Alumina (Al₂O₃)

High alumina contents are highly associated with argillaceous and clayey sediments. The average content of alumina in the studied shales of the different location are 29.09% for Mamu shales and 28.28% for the Nkporo Group.

Alumina (Al₂O₃) has a weak positive trend in the scatter plots of Al₂O₃ vs SiO₂, this is reflected in the correlation matrix of $0.2 \leq r \leq 0.5$ in all the locations with the exception of $r=0.75$ ($r^2=56\%$) at TE. Alumina (Al₂O₃) has a strong negative correlation with TiO₂ of $r = -$

0.82 ($r^2=0.67\%$) at Onyeama Mine and $r = -0.98$ ($r^2 = 96\%$) at Ozalla Junction (FCJ). This may be explained by a considerable amount of detrital inputs from different sources that gave rise to the clay content of the shales.

Calcium (CaO)

The average content of CaO in the studied shale samples are 1.09% and 2.3% for Mamu and Nkporo Group respectively.

These are within those of Mostafa (2005) who investigated the Campanian-Maastrichtian Abu Tartur shales and gave his average as 1.06% and are lower than the average shales as presented by PettiJohn (1975) which are 3.15%. However, the scatter plots of CaO with K₂O, MgO and Na₂O show a negative trend (Fig 3 & 4). This is corroborated by the strong negative correlation matrix of $r = -0.96$ ($r^2 = 92\%$) and $r = -0.88$ ($r^2 = 77\%$) for CaO Vs K₂O and CaO Vs Na₂O respectively at Onyeama Mine and $r = -0.93$ (86%) at FCJ (Ozalla Junction) for CaO Vs MgO. This shows that they do not cohere which indicates different source of origin in relation to the different elements. Therefore CaO can be said to have been formed by a biochemical origin, while K₂O, MgO and Na₂O are of terrigenous origin (inorganic). CaO may be used as marine indicator because, marine shales often have predominantly more calcium than the non-marine ones (Refaat, 1993). As a result the shales from the studied locations can be said to have been from a marginal marine environment because of the low CaO content

Titanium Oxide (TiO₂)

The average titanium oxide content of the studied shale samples is 2.64% and 4.08% for Mamu and Nkporo Group shales respectively. This is higher than that of the shales studied by Mostafa (2005) of 1.04%. Although the scatter plots of TiO₂ with Al₂O₃ show some positive tendency for Mamu shales and Nkporo Group shales, the correlation matrix showed very strong negative correlation with $r = -0.82$ (67%) and $r = -0.98$ (96%) at Onyeama mine and Ozalla Junction (FCJ) respectively. Therefore TiO₂ which is usually associated with clays e.g. Rutile and Anatase according to Degens (1965). can be said to be

terrigenous, but originating from different sources.

Tectonic Setting

The sandstone discriminant function diagram of Bhatia (1983) is based on a bivariate plot of first and second discriminate functions of major element analysis. The plots represent four different tectonic settings which are OIA (Oceanic Island Arc), Continental Island Arc (CIA), Active Continental Margin (ACM), Passive Margin (PM). The functions and the plotting coordinates are from Bhatia (1983). For the Mamu Formation and Nkporo Group sediments, the samples all fall within and around the CIA field with possible contribution from other sources, margins, from the cross plots of Al_2O_3/SiO_2 vs $Fe_2O_3 + MgO$ (Figs 12).

Predictively, one would assume that the tectonic setting of the studied area would be predominantly of a passive margin (PM) since the Anambra Basin was a fall out of the rifted Benue Trough, but the evolution of the basin itself has had significant influence on the sediment geochemistry in that the Tectonic setting being that of CIA. According to Rollison (1993), Continental Island Arcs are inter-arc, fore-arc or back-arc basins, adjacent to a volcanic-arc developed on thick continental crust or thin continental margins.

Peridotite melting leads to the formation of basalts, although low-percent partial melts formed at shallow mantle levels (typically not applicable to continental arcs) can, under certain circumstances, generate basaltic andesites or high-Mg andesites according to Ducea *et al* (2015), Brominates-which are rare, Mg-rich rocks; may be primitive andesites derived by direct melting. Basalts are basic igneous rocks; this agrees with the TiO₂ Vs Ni bivariate plots (Fig 9 & 10).

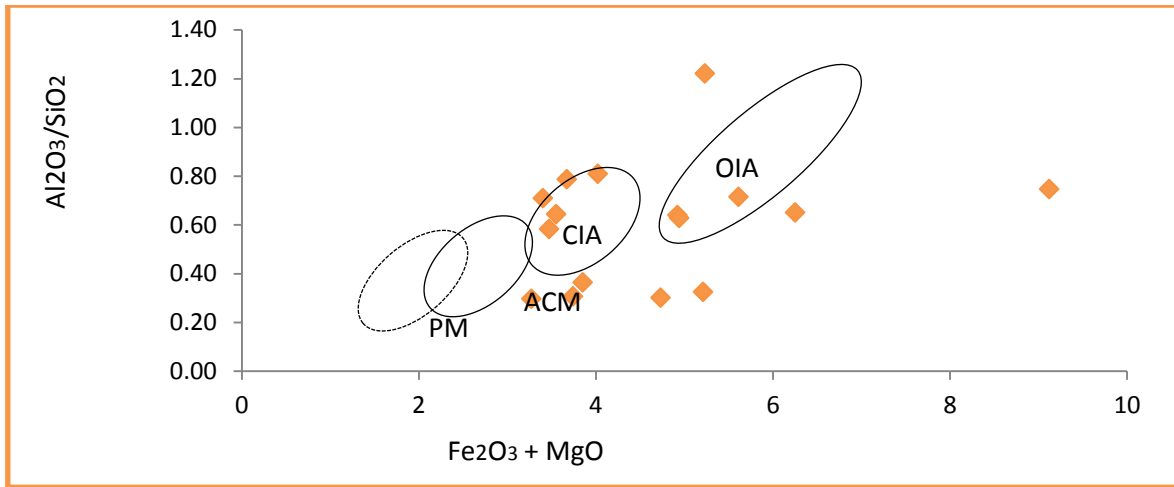


Figure 8: Cross-plots of Enugu Fm

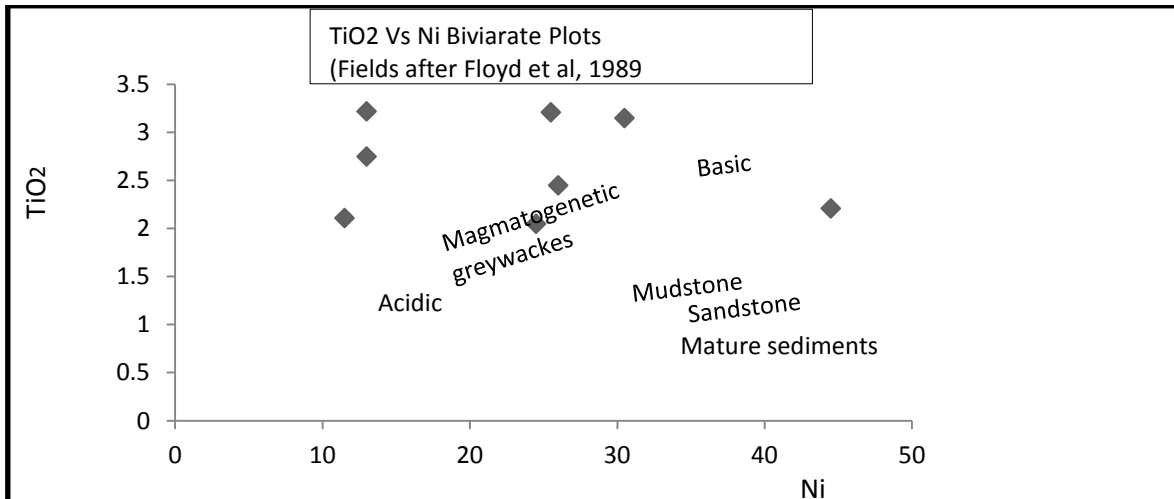


Figure 9: Bivariate plot for Mamu Fm

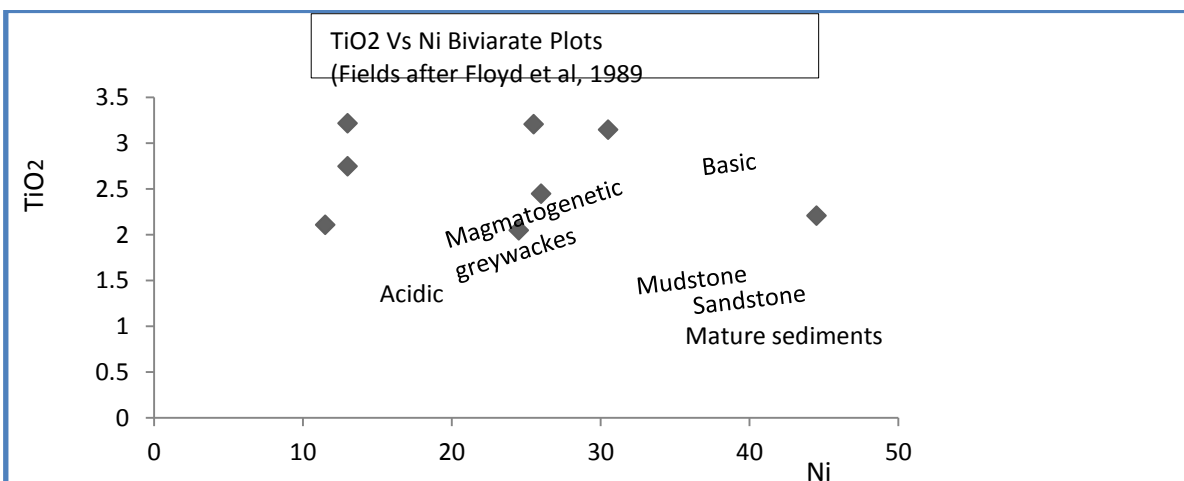


Figure 10: Bivariate plot for Enugu Fm

Provenance

The geochemical signatures of clastic sediments have been used to ascertain provenance characteristics (Taylor and McLennan, 1985; Condie et al., 1992, Cullers, 1995; Armstrong-Altrin et al. 2004).

For most clastic rocks Al_2O_3/TiO_2 ratios are essentially used to infer source rocks composition because Al_2O_3/TiO_2 ratios increase from 3 to 8 for mafic igneous rock, from 8 – 21 for intermediate rocks and from 21 to 70 for felsic igneous rocks (Hayashi et al, 1997). The Al_2O_3/TiO_2 range from 7.69 - 14.99 and 5.41 – 8.04 for Mamu and Nkporo Group shales respectively. This indicates that the Mamu shales are mostly from intermediate igneous rocks, while the Nkporo Group are predominantly from mafic igneous rocks. This corroborates the results of the discriminant functions plots in that all the samples fall within the CIA (Continental Island Arc) region. The CIA and OIA are characterized by basalt–andesite-rhyolite associations, which are predominantly basic rocks to intermediate igneous rocks and then felsic rocks. The origin of basalts and basaltic andesites in arcs has unresolved details (Grove et al. 2012) but is fairly well understood. However, continental arcs are on average more silicic than basalt, and therefore require an additional step in their magmatic evolution (Rudnick 1995).

Elemental concentrations in sediments result from the competing influences of provenance, weathering, sorting, and sediment diagenesis (Quinby-Hunt et al., 1991). The studied shales show generally enrichment of elements that are chemically resilient and are associated with terrigenous influx, such as SiO_2 , Al_2O_3 and TiO_2 . SiO_2 , Al_2O_3 and TiO_2 that can survive throughout

intensive chemical weathering and diagenesis (Cullers, 2000). Therefore their concentration in sediments is used as a measure of detrital input. The major constituents of the studied shale samples do not vary greatly from one location to another. The SiO_2 , Al_2O_3 and TiO_2 tend to form together the main constituents of the studied shales and are normally related to clays. SiO_2 , Al_2O_3 and TiO_2 show both strong positive and negative correlation in most of the samples. This indicates that the major constituents SiO_2 , Al_2O_3 and TiO_2 of the studied shale samples are dominantly terrigenous in origin but might have originated from different sources. The tectonic setting indicated Continental Island Arc source with possible contribution from other tectonic setting such as the Oban Massif. The provenance indicates that the sediments were from a mixed source of felsic and mafic parent rocks.

REFERENCES

- Agumanu, A.E. (1993). Sedimentology of Owelli Sandstone (Campano-Maastrichtian), southern Benue trough, Nigeria. *Journal of Mineralogy and Geology*, 29(2), p. 21-25.
- Ahmed, H. A. (1997). Mineralogical and geochemical studies of the black shales intercalated with phosphorite deposits at Abu Tartur area Western Desert, Egypt: M.Sc. thesis, Ain Shams Uni. Cairo, Egypt, p.284.
- Armstrong-Altrin, J.S., Lee, Y.I., Verma, S.P., Ramasamy, S. (2004). Geochemistry of sandstones from the upper Miocene Kudankulam Formation, southern India: Implications for provenance,

- weathering, and tectonic setting: *Journal of Sedimentary Research*, 74(2), p.285-297.
- Bain, D.C. and Smith, B.F.L. (1987). Chemical Analysis; In: A Handbook of Determinative Methods in Clay Mineralogy, WILSON, M.J. (Ed). p 248-274.
- Bhatia, M.R. (1983). Plate tectonics and geochemical composition of sandstones: *Journal of Geology*, 91, p.611-627.
- Condie, K.C., Boryta M.D., Liu J., Quian X. (1992). The origin of khondalites: geochemical evidence from the Archean to Early Pro-terozoic granulitic belt in the North China Craton: *Precambrian Research*, 59(3-4), p.207-223.
- Cullers, R.L. (1995). The controls on the major and trace element evolution of shales, siltstones and sandstones of Ordovician to Tertiary age in the Wet Mountain region, Colorado, U.S.A: *Chemical Geology*, 123(1-4), p.107-131.
- Degens, E.T. (1965): *Geochemistry of sediments: A brief survey* Prentice-hall, New Jersey.
- Ducea, M.N Jason B. Saleeby, George Bergantz (2015). The Architecture, Chemistry, and Evolution of Continental Magmatic Arcs. *The Annual Review of Earth and Planetary Science*. 43:10.1–33p
- Felix, N.S. (1977): Physico-chemical studies on bentonites with special reference to Fayoum Deposits, in: Mostafa, G.M.A.T (2005). Mineralogical and geochemical studies of carbonaceous shale deposits from Egypt. *Published Ph.D.Thesis, Technical University of Berlin*, p 48-78.
- Grove TL, Till CB, Krawczynski MJ. 2012. The role of H₂O in subduction zone magmatism. *Annu. Rev. Earth Planet. Sci.* 40:413p.
- Hayashi, K., Fujisawa, H., Holland, H., Ohmoto, H. (1997) Geochemistry of 1.9 Ga Sedimentary rocks from northeastern Labrador- Canada. *Geochimica et Cosmochimica Acta* 61 (19) p 4115 – 4137.
- Moore, D.M. and Reynolds, R.C. Jr. (1997). X-Ray diffraction and the Identification and Analysis of Clay Minerals. *Oxford University Press, New York*, 378 pp.
- Mostafa, G.M.A.T (2005). Mineralogical and geochemical studies of carbonaceous shale deposits from Egypt. *Published Ph.D.Thesis, Technical University of Berlin*, p 48-78.
- Nwajide, C.S. and Reijers, T.J.A. (1997). Sequences Architecture of the Campanian Nkporo and the Eocene Nanka Formation of the Anambra Basin, Nigeria, In: Reijers, T. J. A., (ed). *Selected Chapters on Geology. Warri: SPDC*, p. 133-148.
- Nwajide, C.S and Reijers, T.J.A. (1996). The Geology of the Southern Anambra Basin, in: T.J.A. Reijers (ED.) *selected chapter in Geology*

- sedimentary geology and sequence stratigraphy of the Anambra Basin, *SPDC publication*, p. 133-148.
- Obaje, N.G., Wehner, H., Scheeder, G., Abubakar, M.B., and Jauro, A. (2004). Hydrocarbon Prospectivity of Nigeria Inland Basin: From the Viewpoint of Organic Geochemistry and Organic Petrography. *AAPG Bulletin*, V.88, p.325-353.
- Ofoegbu, C.O., Odigi, M.I., and Ebeniro, J.O. (1990). On the Tectonic Evolution of the Benue Trough. In: Ofoegbu, C.O. (Ed): The Benue Trough Structure and Evolution; *Int. Earth Sci. Mono. Series, Vieweg and Soln, Wiesbaden Germany*, p.208 - 216.
- Pettijohn, F.J. (1975). *Sedimentary Rock* (3 ed) Harper and Row, New York. 628p.
- Quinby-Hunt, M.S., Wilde, P and Berry W.B. N (1991) The provenance of low – calcic black shales *Minerallium Deposita* 26 p113 – 121.
- Refaat, A.A. (1993). Facies Development of the Coniacian-Santonian Sediments along the Gulf of Suez, Egypt, in: Mostafa, G.M.A.T (2005). Mineralogical and geochemical studies of carbonaceous shale deposits from Egypt. *Published Ph.D.Thesis, Technical University of Berlin*, p 48-78.
- Rollison R. H, (1993). Using geochemical data: Evaluation, Presentation, Interpretation, *Longman Scientific & Technical*, PP 206-210.
- Rudnick RL. 1995. Making continental crust. *Nature* 378:p571–578
- Sharma, G.D. (1979): *The Alaskan Shelf*. Spriger-Verlag, New York, in: Mostafa, G.M.A.T (2005). Mineralogical and geochemical studies of carbonaceous shale deposits from Egypt. *Published Ph.D.Thesis, Technical University of Berlin*, p 48-78.
- Taylor, S.R., and McLennan S., (1985). *The Continental Crust: Its Composition and Evolution*: Blackwell, Oxford, 312 p.
- Whiteman, A.J. (1982). *Nigeria: Its Petroleum Geology, Resources and Potentials*. V. I and II London, Graham and Trotman, 381p.